BIOCHEMISTRY
including biophysical chemistry & molecular biology

Article

pubs.acs.org/biochemistry

Allosteric Modulation of Substrate Motion in Cytochrome P450 3A4-Mediated Xylene Oxidation

W. Kurtis Childers[†,§] and John P. Harrelson*[,‡]

[†]Chemistry Department, Pacific University Oregon, Forest Grove, Oregon 97116, United States

[‡]School of Pharmacy, Pacific University Oregon, Hillsboro, Oregon 97123, United States

Supporting Information

ABSTRACT: Many cytochrome P450 enzymes (CYPs) exhibit allosteric behavior reflecting a complex ligand-binding process involving numerous factors: conformational selection, protein−protein interactions, substrate/effector/protein structure, and multiple-ligand binding. The interplay of CYP plasticity and rigidity contributes to substrate/product selectivity and to allosterism. Detailed evidence describing how protein motion modulates product selectivity is incomplete as are descriptions of effector-induced modulation of substrate dynamics. Our intent was to discover details of allosteric behavior and CYP3A4 flexibility and rigidity by investigating substrate motion using low-molecular weight ligands. Steady state kinetics and product ratios were measured for oxidation of *m*-xylene-$^2H_3$ and *p*-xylene; intramolecular isotope effects were measured for *m*-xylene-$^2H_3$ oxidation as a function of *m*-xylene-$^2H_3$ and *p*-xylene concentration. Biphasic kinetic plots indicated homotropic cooperative behavior with xylene isomers. Selectivity for aromatic hydroxylation over benzylic hydroxylation of *m*-xylene-$^2H_3$ supports a model in which the region near the CYP3A4 active oxidizing species limits substrate dynamics. *p*-Xylene impedes the motion of *m*-xylene-$^2H_3$ substrates that have access to the active oxidizing species: $(k_H/k_D)_{obs}$ values for *m*-xylene-$^2H_3$ decreased with *p*-xylene concentration. *m*-Xylene-$^2H_3$ and *p*-xylene do not have simultaneous access to the active oxidizing species: deuterium-labeled and unlabeled *p*-xylene exhibited similar effects on the $(k_H/k_D)_{obs}$ values for *m*-xylene-$^2H_3$ oxidation. *p*-Xylene and *m*-xylene-$^2H_3$ bind at different sites: *m*-xylene-$^2H_3$ oxidation rates and product selectivity were consistent across the *p*-xylene concentration range. Overall, this study indicates that the intramolecular isotope effect experimental design provides a unique opportunity to investigate allosteric mechanisms as it provides information about substrate motion when the enzyme is primed to oxidize substrates.

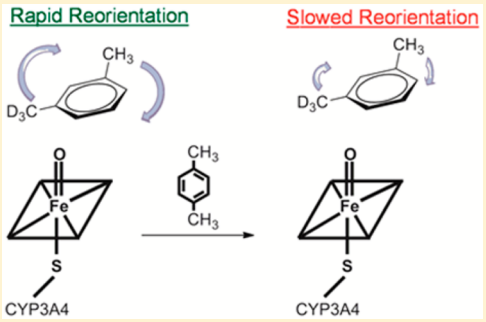

Cytochrome P450 enzymes (CYP) make up a superfamily of enzymes present in many eukaryotes and prokaryotes that metabolize both endogenous and exogenous compounds, usually through oxidative chemistry. CYP enzymes are remarkably diverse in their relevance to biology, playing important roles in toxicity, synthetic pathways, drug clearance, and drug−drug interactions and acting as therapeutic targets. Such diverse function is reflected in complex enzymatic and biochemical behavior. Many CYP isoforms exhibit a profound capacity to accommodate substrates of wide structural diversity and to catalyze a variety of chemical reaction types.[1,2] There are also countless examples of product promiscuity wherein a single CYP isoform catalyzes the formation of multiple products from the same substrate.[3,4]

A mechanistically intriguing phenomenon observed with many CYP enzymes is a novel type of allosteric modulation. While several methods have been used to identify this behavior, it is often identified by kinetic plots that deviate from the Michaelis−Menten model.[5] Initially, the activation of CYP-mediated metabolism was reported;[6−8] however, it does not necessarily result in positive binding cooperativity. It can also lead to functional changes, for example, modulation of product selectivity,[9] negative cooperativity, or substrate inhibition.[10] For the sake of clarity, the term "ligand" is defined here as a molecule that binds to the enzyme, which could be at a peripheral site without access to the active oxidizing species or within the active site with access to the active oxidizing species. The term "substrate" is used throughout to specify a ligand that binds to the enzyme but also has access to the active oxidizing species and is ultimately metabolized to a product. An "effector" ligand may not have access to the active oxidizing species but still modulate the product selectivity for substrate metabolism.

The type of allosteric modulation observed in CYP enzymes is ligand- and isoform-dependent and thus highly unpredictable based on current models. While the experimental conditions necessary to unequivocally observe allosteric behavior limit its observation,[11] *in vivo* allosteric modulation has been detected in several species, including humans.[12−15] It can complicate *in vitro*−*in vivo* predictions, which are routinely conducted to evaluate potential drug−drug interactions and drug clear-

Received: October 29, 2013
Revised: January 24, 2014
Published: January 29, 2014

   dx.doi.org/10.1021/bi401472p | *Biochemistry* 2014, 53, 1018−1028

ance.[16,17] Fluconazole modulates the metabolite profile of midazolam in humans,[3] prompting suggestions that heterotropic effects be investigated more extensively during drug−drug interaction studies.[18]

The mechanistic basis for allosteric and cooperative behavior in CYPs is varied and complex.[5,9,19−22] Briefly, it can involve multiple ligands binding simultaneously, the existence of distinct conformers of a single isoform, and/or the formation of protein−protein complexes. In the case of multiple-ligand binding, molecules can bind simultaneously near the heme, wherein the ligands may interact with one another in addition to the CYP protein.[23] Alternatively, the "effector" ligand may bind at a distant site away from the heme.[24,25] Protein motion and the interplay between plasticity and rigidity contribute to the complexity of predicting allosteric phenomena and substrate/product selectivity.[26−33] Solid state nuclear magnetic resonance,[34] stopped-flow,[35,36] and crystallographic experiments[28] all have indicated that substrate binding is a dynamic process; however, little is known about how the motion of a substrate with access to the active oxidizing species is modulated by allosteric and cooperative phenomena. Thus, one goal of this study was to investigate the role of substrate dynamics in CYP allosteric behavior.

Intramolecular isotope effect experiments have been utilized to study a variety of CYP phenomena.[37−45] Experiments with substrates that contain symmetrically related methyl groups, such as *m*-xylene-$^2H_3$ (Figure 1), provide a method for studying

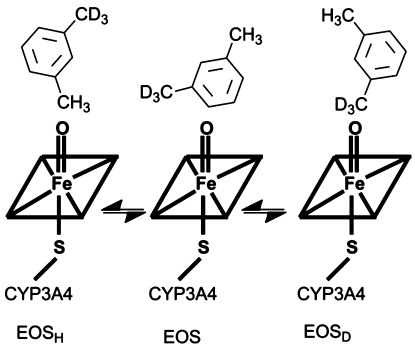

Figure 1. Theoretical illustration demonstrating how the substrate must be oriented relative to the active oxygen species to achieve EOS_H and EOS_D.

substrate dynamics.[37,38,45−47] For example, in CYP2A6, the motion of *m*-xylene-$^2H_3$ substrate molecules slowed in the presence of *p*-xylene. Moreover, the product ratio (*m*-methylbenzyl alcohol to 2,4-dimethylphenol) for CYP2A6-mediated oxidation of *m*-xylene-$^2H_3$ shifted profoundly when it was co-incubated with *p*-xylene (i.e., 7.2 ± 0.6 in the absence of *p*-xylene and 2.4 ± 0.2 with 200 μM *p*-xylene) (Figure 2). A

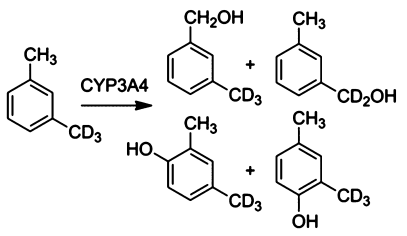

Figure 2. CYP3A4-mediated formation of *m*-methylbenzyl alcohol and 2,4-dimethylphenol products from *m*-xylene-α-$^2H_3$ oxidation.

benefit of this experimental design is that it provides information about substrate motion when the enzyme is primed to oxidize substrates. There are many tools for investigating CYPs when they are in a resting or semiresting state. However, the complexity of ligand binding and possible changes in CYP−ligand interactions at different steps along the reaction cycle generate ambiguity with respect to how results generated from experiments with the resting state apply to the CYP enzyme when it is in an active oxidizing state, especially when multiple ligands are involved.[48−51]

CYP3A4 is an excellent candidate for investigating the role of substrate dynamics in allosterism because of vast reports of such behavior. CYP3A4 also exhibits broad substrate selectivity and accommodates higher-molecular weight substrates. All these characteristics are often attributed to great protein flexibility.[26,27,29] However, even this most malleable of CYP enzymes exhibits product selectivity, which points to protein rigidity having a role in determining the ultimate site of oxidation.[26] Thus, a second goal of this study was to investigate the limits of CYP3A4's flexibility and rigidity by utilizing low-molecular weight ligands to investigate allosteric behavior. Although there are a few studies with low-molecular weight ligands,[48,52] studies of CYP3A4 have predominantly focused on interactions with higher-molecular weight ligands, for example, in the range of 160−480 Da[53−55] and even higher, such as erythromycin, which have provided a sense of CYP3A4's flexibility to expand and to accommodate multiple ligands simultaneously.[27] We postulated that experiments with low-molecular weight ligands would provide information about CYP3A4's flexibility in another sense, that is, to contract to a degree that substrate approach and/or motion will be sterically hindered by enzyme residues. To investigate this and the role of substrate dynamics in allosteric behavior, we investigated two hypotheses. (1) CYP3A4-mediated metabolism of xylene isomers will exhibit homotropic and heterotropic cooperative behavior. (2) Allosteric behavior during CYP3A4-mediated oxidation of *m*-xylene-$^2H_3$ will modulate substrate motion as indicated by changes in intramolecular isotope effect values, $(k_H/k_D)_{obs}$, and product ratios for benzylic and aromatic hydroxylation routes.

EXPERIMENTAL PROCEDURES

Materials. The synthesis and characterization of *m*-xylene-α-$^2H_3$ have been described previously.[46] Supersomes (human CYP3A4 with P450 reductase and cytochrome b_5) and insect cell control microsomes were from BD Gentest. *p*-Xylene, *p*-xylene-α,α,α,α′,α′,α′-$^2H_6$, pentane, *N*,*O*-bis(trimethylsilyl)-trifluoroacetamide (BSTFA), β-nicotinamide adenine dinucleotide 2′-phosphate reduced sodium salt (NADPH), *m*-methylbenzyl alcohol, 2,4-dimethylphenol, 2,5-dimethylphenol, 3,4-dimethylphenol, and *p*-methylbenzyl alcohol were purchased from Sigma-Aldrich. The SHR5XLB gas chromatography capillary column (30 mm × 0.25 μm × 0.25 mm) was purchased from Shimadzu (Kyoto, Japan).

Kinetic Experiments and Product Ratio Quantitation for the Hydroxylation of *m*-Xylene-α-$^2H_3$ and *p*-Xylene by CYP3A4. Determination of the Intramolecular $(k_H/k_D)_{obs}$ for *m*-Xylene-α-$^2H_3$ Hydroxylation. *m*-Xylene-α-$^2H_3$ (6−1000 μM) or *p*-xylene (6−1000 μM) dissolved in methanol and CYP3A4 Supersomes (30−100 pmol) were preincubated in borosilicate glass test tubes (16 mm × 150 mm, volume of 22 mL) for 3 min at 37 °C in incubation buffer [100 mM potassium phosphate (pH 7.4)]. The final concentration of

dx.doi.org/10.1021/bi401472p | *Biochemistry* 2014, 53, 1018−1028

methanol in all samples was 1%. Incubations (600 μL) were initiated by the addition of NADPH (1 mM), proceeded for 6 min at 37 °C, and then were terminated by the addition of ice-cold pentane (3 mL) followed by the addition of the internal standard (100 pmol of 3,4-dimethylphenol dissolved in methanol). The incubation period was determined by measuring product formation as a function of time at high and low substrate concentrations. Following a second extraction with 3 mL of pentane, the organic layers were combined and dried with magnesium sulfate, which was removed by centrifugation. The pentane layers were transferred to a glass evaporation tube (18 mm × 115 mm, volume of 19.5 mL, narrow tapered bottom) and evaporated to approximately 75 μL with compressed air. The hydroxylated metabolites were derivatized by the addition of 20 μL of a BSTFA/ethyl acetate mixture (1/1) and heated at 50 °C for 20 min. The derivatized samples were then analyzed by gas chromatography and mass spectrometry (GC–MS). Experiments with *m*-xylene-α-$^2H_3$ and *p*-xylene were conducted in quadruplicate and triplicate, respectively. For example, data points in Figures 3–5 are the average of four independent experimental samples generated over a period of 4 days. Controls included incubations with high substrate concentrations without the addition of CYP3A4 Supersomes. All substrate and internal standard additions were conducted using positive displacement pipettes.

Heterotropic Experiments: Determination of Product Ratios and Intramolecular $(k_H/k_D)_{obs}$ Values for CYP3A4-Mediated Oxidation of *m*-Xylene-α-$^2H_3$ in the Presence of Unlabeled and Deuterium-Labeled ($^2H_6$) *p*-Xylene. These experiments were conducted like the studies described above with some minor variations. *m*-Xylene-α-$^2H_3$ (50 μM) and unlabeled *p*-xylene or deuterium-labeled *p*-xylene-$^2H_6$ (10–500 μM) were preincubated with CYP3A4 Supersomes (30 pmol) for 3 min at 37 °C in incubation buffer [100 mM potassium phosphate (pH 7.4)]. Substrate and effector molecules were dissolved in methanol (final concentration in incubations of 1%). Incubations (600 μL) were initiated by the addition of NADPH (1 mM), proceeded for 6 min at 37 °C, and then were terminated by the addition of ice-cold pentane (3 mL) followed by the addition of the internal standard (100 pmol of 3,4-dimethylphenol dissolved in methanol). Extraction, drying, and derivitization were the same as described above. Experiments were conducted in quadruplicate (i.e., four independent samples) and triplicate for unlabeled and deuterium-labeled *p*-xylene, respectively.

Kinetic Analysis. Nonlinear regression (GraphPad Prism 5, GraphPad, San Diego, CA) was used to analyze the kinetic data. Velocities for individual metabolites and total product were plotted as *v* versus *v*/[substrate] and also fit to a two-enzyme model and a two-active site model[56] to evaluate the prospect of allosteric behavior and to generate K_{m1} values to determine appropriate *m*-xylene-α-$^2H_3$ and *p*-xylene concentrations for heterotropic experiments. Fits to the Michaelis–Menten model were also evaluated.

Quantitation of Xylene Metabolites by GC–MS. Derivatized metabolites were analyzed with a Shimadzu GC-2010 gas chromatograph equipped with a Shimadzu SHR5XLB column (30 m × 0.25 μm × 0.25 mm) and interfaced with a Shimadzu 2010S mass spectrometer. Xylene metabolites were injected (injection temperature of 250 °C) on the column at an oven temperature of 40 °C and eluted with a linear gradient of 6 °C/min to 105 °C, 3 °C/min to 122 °C, and 25 °C/min to 250 °C for a total run time of 23.62 min. The mass spectrometer was operated in the electron impact mode at a −70 eV electron energy with source and interface temperatures set at 260 and 250 °C, respectively. Ions were detected in the selected ion monitoring mode. Monitored ions corresponded to the $[M - 15]^+$ fragments generated from the trimethylsilated hydroxyl metabolites. Metabolite retention times were confirmed by comparison to retention times of commercially available standards. Isotope effect values were calculated using the peak areas of ions at *m*/*z* 180, 181, 182, and 183 to correct for natural isotopic abundance and incomplete deuterium incorporation as previously described.[46] Metabolite quantification was conducted by generating standard curves using unlabeled standards. Representative standard curves and chromatograms are available in the Supporting Information. The lower limit of detection for all metabolites was 5 pmol/600 μL incubation volume. The metabolite concentrations in all experimental samples exceeded this lower limit.

RESULTS

Experimental Rationale for Measurement of the Intramolecular Isotope Effect and Product Ratios. The observed intramolecular isotope effect, $(k_H/k_D)_{obs}$, for *m*-xylene-$^2H_3$ oxidation is measured by determining the ratio of products formed from hydroxylation at the unlabeled and deuterium-labeled methyl groups of *m*-xylene-$^2H_3$. That is

$$(k_H/k_D)_{obs} = P_H/P_D =$$

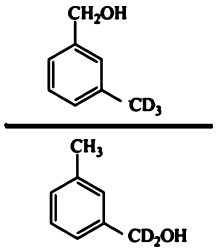

Two modulators of the observed intramolecular isotope effect are the formation of multiple products (i.e., metabolic switching) and the rate of substrate reorientation. The theory that describes how these two factors influence the observed intramolecular isotope effect has been developed and is described by Scheme 1 and eq 1.[39,57−59]

In this scheme, EOS_H and EOS_D represent *m*-xylene-$^2H_3$ bound to CYP3A4 with the unlabeled and deuterium-labeled methyl group oriented toward the active oxidizing species, respectively (Figure 1). Similarly, the terms k_{45H} and k_{45D} represent the rate constants for oxidation at the unlabeled and deuterium-labeled methyl groups, respectively.

$$(k_H/k_D)_{obs} = \frac{k_{45H}/k_{45D} + k_{45H}/(k_{43} + k_{46})}{1 + k_{45H}/(k_{43} + k_{46})} \quad (1)$$

This equation describes how the measured isotope effect, $(k_H/k_D)_{obs}$, changes as a function of the reorientation rate (k_{43}) and the rate of metabolism at a "switch to" site that is not isotopically labeled (k_{46}).

While the intrinsic isotope effect for benzylic oxidation, k_{45H}/k_{45D}, is independent of the rate of reorientation (k_{43}) between the labeled and unlabeled methyl groups, the experimentally determined isotope effect, $(k_H/k_D)_{obs}$, is profoundly influenced by the rate of reorientation. Thus, changes in the measured isotope effect indicate changes in the rate of substrate

dx.doi.org/10.1021/bi401472p | Biochemistry 2014, 53, 1018–1028

Scheme 1. Rate Constants and Potential Products Generated from an Intramolecular Isotope Effect Experiment[a]

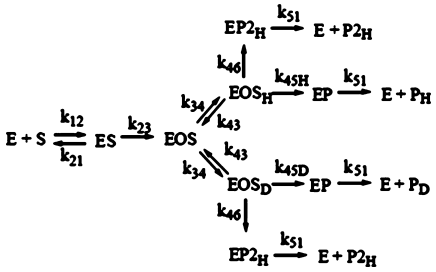

[a]In the case of *m*-xylene-$^2H_3$, P_D and P_H represent *m*-methylbenzyl alcohol formed from hydroxylation at the deuterium-labeled and unlabeled methyl groups, respectively. $P2_H$ represents formation of 2,4-dimethylphenol, a "switch to" site that is not isotopically labeled and is not symmetrically related to the methyl groups. Two rate constants modulate the value of $(k_H/k_D)_{obs}$: the rate reorientation (k_{43}) between the labeled and unlabeled methyl groups and the rate of metabolism at the switch to site (k_{46}).

reorientation. If the rate of reorientation is rapid relative to the rate of oxidation, then the measured isotope effect will approach the intrinsic isotope effect; when the rate of reorientation is slow, then the measured isotope effect, $(k_H/k_D)_{obs}$, decreases.[37,38] Thus, changes in the measured isotope effect can indicate changes in the rate of substrate reorientation when effects on uncoupling and metabolic switching are also considered. For allosteric phenomena, this experimental design provides a tool for investigating how effector ligands influence substrate motion.

A slow reorientation rate does not necessarily mean that the $(k_H/k_D)_{obs}$ will decrease if there is an alternate site available for oxidation that generates $P2_H$ (k_{46}).[57−59] Values of $(k_H/k_D)_{obs}$ can approach the intrinsic isotope effect if k_{46} is substantial. In the case of *m*-xylene-$^2H_3$, k_{46} and $P2_H$ refer to the formation of 2,4-dimethylphenol generated via metabolic switching from benzylic hydroxylation to aromatic hydroxylation (Figure 2). The overall effect on $(k_H/k_D)_{obs}$ is dependent on $\Delta k_{43}/\Delta k_{46}$. There are two scenarios indicative of a decrease in the level of substrate reorientation as a function of ligand concentration. In the first, $(k_H/k_D)_{obs}$ values decrease while the product ratio (e.g., 2,4-dimethylphenol/*m*-methylbenzyl alcohol) is steady across the concentration range. Alternatively, $(k_H/k_D)_{obs}$ values are consistent across the concentration range while the level of formation of $P2_H$ increases.[44]

Kinetic Analysis of CYP3A4-Mediated Oxidation of *m*-Xylene-$^2H_3$. 2,4-Dimethylphenol and *m*-methylbenzyl alcohol were the major products generated from the CYP3A4-mediated metabolism of *m*-xylene-$^2H_3$ (Figure 2) with selectivity for 2,4-dimethylphenol. Eadie−Hofstee plots (v vs $v/[S]$) generated for total product, 2,4-dimethylphenol, and *m*-methylbenzyl alcohol products were biphasic (Figure 3). Rates for total product formation were fit to a two-enzyme model and a two-active site model[56] to estimate K_{m1} to select a substrate concentration for the heterotropic studies that followed. Both models generated the same K_{m1} (95 μM). The curves for the two models were essentially identical with V_{max1} values of 2.2 and 2.4 pmol min^{-1} pmol^{-1}. Figure 4 displays the curve generated from fitting to the two-enzyme model.

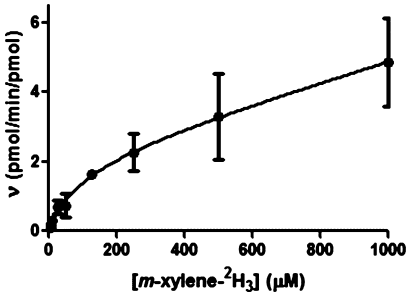

Figure 4. Rates of total product formation for CYP3A4-mediated oxidation of *m*-xylene-$^2H_3$ fit to a two-enzyme (i.e., biphasic) kinetic model.

Product Ratio and Intramolecular Isotope Effect $(k_H/k_D)_{obs}$ Values for CYP3A4-Mediated Oxidation of *m*-Xylene-$^2H_3$. The product ratio (2,4-dimethylphenol/*m*-methylbenzyl alcohol) increased with substrate concentration from 0.93 ± 0.36 at 6 μM *m*-xylene-$^2H_3$ to a high of 3.20 ± 0.44 at 500 μM *m*-xylene-$^2H_3$ (average ratio across all concentrations of 2.31 ± 0.73) (Figure 5). The concentration-dependent increase in the product ratio was mirrored in the $(k_H/k_D)_{obs}$ values, consistent with Scheme 1 and eq 1.

CYP3A4-Mediated Oxidation of *p*-Xylene. CYP3A4 exhibited product selectivity for *p*-methylbenzyl alcohol over 2,5-dimethylphenol (Figures 6 and 7). As seen for *m*-xylene-$^2H_3$, Eadie−Hofstee plots for total product formation and individual products were biphasic (Figure 8). Rates for total product formation were fit to a two-enzyme model[56] to estimate K_{m1} to select a low-end effector concentration for the heterotropic studies. The values of V_{max1} and K_{m1} were 0.37 pmol min^{-1} pmol^{-1} and 54 μM, respectively. The curve generated from fitting to the two-enzyme model, similar to Figure 4 for *m*-xylene-$^2H_3$, is available in the Supporting Information. The product ratio (*p*-methylbenzyl alcohol/2,5-dimethylphenol) was consistent across the substrate concentration range, with an average of 2.9 ± 0.6 (Figure 7).

Heterotropic Effects of *p*-Xylene and *p*-Xylene-$^2H_6$ on CYP3A4-Mediated *m*-Xylene-$^2H_3$ Oxidation. Heterotropic effects were observed on $(k_H/k_D)_{obs}$ values, which decreased

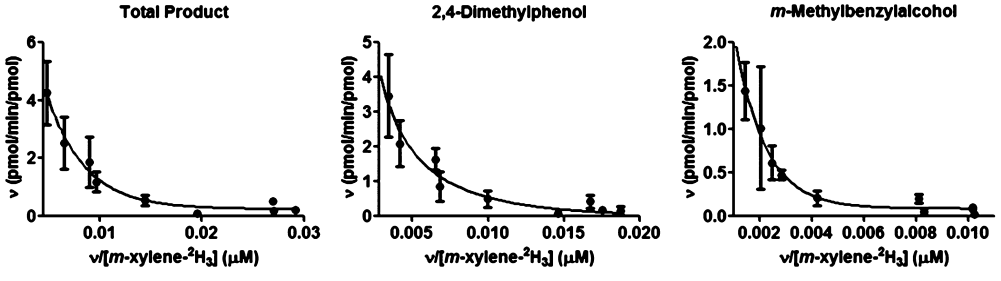

Figure 3. Eadie−Hofstee plots for the CYP3A4-mediated oxidation of *m*-xylene-$^2H_3$.

dx.doi.org/10.1021/bi401472p | *Biochemistry* 2014, 53, 1018−1028

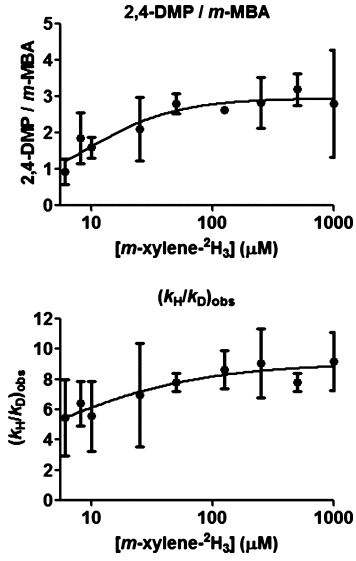

Figure 5. Product ratio (2,4-dimethylphenol/*m*-methylbenzyl alcohol) and intramolecular isotope effect as a function of *m*-xylene-$^2H_3$ concentration.

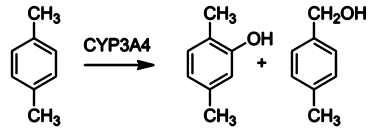

Figure 6. Major products formed from CYP3A4-mediated *p*-xylene oxidation: 2,5-dimethylphenol and *p*-methylbenzyl alcohol.

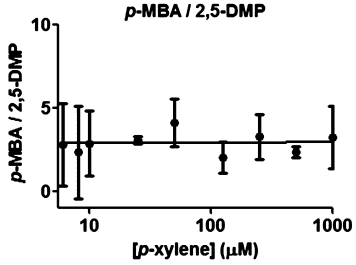

Figure 7. Product ratio (*p*-methylbenzyl alcohol/2,5-dimethylphenol) as a function of *p*-xylene concentration.

with *p*-xylene concentration from a maximum of 8.4 ± 0.5 at 25 μM *p*-xylene to 4.4 ± 1.2 at 500 μM *p*-xylene ($p < 0.001$) (Figure 9 and Table 1). *p*-Xylene-$^2H_6$ exhibited a similar trend: $(k_H/k_D)_{obs}$ = 9.0 ± 0.9 and 6.5 ± 0.5 at 25 and 500 μM *p*-xylene-$^2H_6$, respectively ($p < 0.02$). Overall, the product selectivity for *m*-xylene-α-$^2H_3$ oxidation was similar to that from the homotropic experiments; however, the trends differed

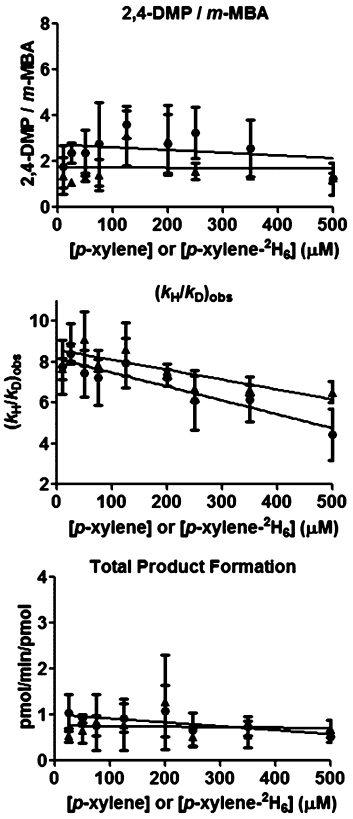

Figure 9. Product ratio (2,4-dimethylphenol/*m*-methylbenzyl alcohol), $(k_H/k_D)_{obs}$, and rate of total product formation for CYP3A4-mediated oxidation of *m*-xylene-$^2H_3$ as a function of *p*-xylene (●) and *p*-xylene-$^2H_6$ concentration (▲). Total product (picomoles per minute per picomole) refers to products formed from *m*-xylene-$^2H_3$.

Table 1. Effects of *p*-Xylene and *p*-Xylene-$^2H_6$ on $(k_H/k_D)_{obs}$ Values for CYP3A4-Mediated Oxidation of *m*-Xylene-$^2H_3$.

substrate and effector	$(k_H/k_D)_{obs}$	pmol min^{-1} pmol^{-1}[a]
50 μM *m*-xylene-$^2H_3$	7.8 ± 0.6	0.72 ± 0.34
with 25 μM *p*-xylene	8.4 ± 0.5	1.04 ± 0.40
with 25 μM *p*-xylene-$^2H_6$	9.0 ± 0.9	0.63 ± 0.08
with 500 μM *p*-xylene	4.4 ± 1.3[b]	0.52 ± 0.11
with 500 μM *p*-xylene-$^2H_6$	6.5 ± 0.5[c]	0.69 ± 0.19

[a]Refers to products formed from *m*-xylene-$^2H_3$. [b]$p < 0.001$ compared to samples containing 25 μM *p*-xylene. [c]$p < 0.02$ compared to samples containing 25 μM *p*-xylene-$^2H_6$.

as a function of concentration. Homotropic experiments exhibited an increase in the product ratio (2,4-dimethylphenol/*m*-methylbenzyl alcohol) as a function of *m*-xylene-α-$^2H_3$

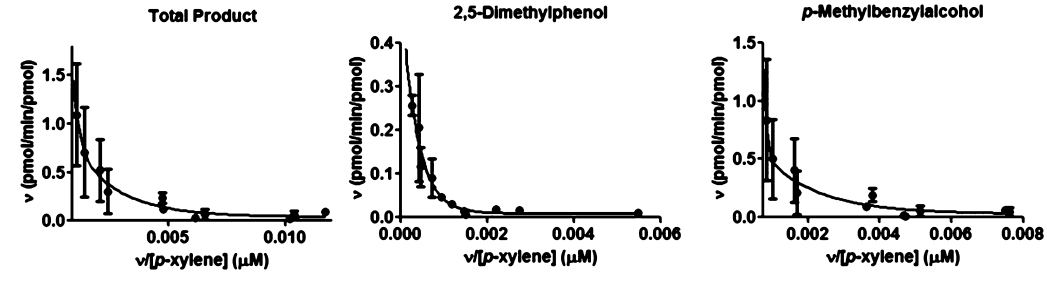

Figure 8. Eadie–Hofstee plots for the CYP3A4-mediated oxidation of *p*-xylene.

dx.doi.org/10.1021/bi401472p | *Biochemistry* 2014, 53, 1018–1028

concentration (Figure 5), while the trend was flat with an increasing *p*-xylene concentration (Figure 9). A decrease in $(k_H/k_D)_{obs}$ in the absence of profound changes in the product ratio (k_{46}) indicates a decrease in the substrate reorientation rate (k_{43}) (Scheme 1 and eq 1).

The trends in the product ratio and $(k_H/k_D)_{obs}$ values for *m*-xylene-α-$^2H_3$ oxidation in the presence of labeled and unlabeled *p*-xylene were similar across all concentrations (Figure 9). Averaged across all effector concentrations, the 2,4-dimethylphenol/*m*-methylbenzyl alcohol ratio equaled 2.5 ± 0.7 and 1.7 ± 0.8 for unlabeled and labeled *p*-xylene, respectively. The turnover of *m*-xylene-$^2H_3$ was not inhibited by the presence of the effector molecules. The average percent activity in comparison to *m*-xylene-$^2H_3$ (50 μM) oxidation in the absence of *p*-xylene effector molecules was 115.7 ± 26.5 and 102.1 ± 33.9% for unlabeled and labeled *p*-xylene, respectively (averaged across all *p*-xylene concentrations). Moreover, the rate of *m*-xylene-$^2H_3$ turnover was consistent across the entire effector concentration range (Figure 9).

DISCUSSION

The results from this study provide new insights into the impact of heterotropic effectors on substrate motion and the spatial rigidity within the region of the active oxidizing species of CYP3A4 with low-molecular weight substrates. CYP3A4 exhibits homotropic and heterotropic cooperative behavior with low-molecular weight xylene isomers. CYP3A4-mediated oxidation of *m*-xylene-$^2H_3$ surprisingly displayed selectivity for aromatic hydroxylation over benzylic hydroxylation. This supports a model in which the heme binding core is rigid.[26] That is, while CYP3A4 exhibits great flexibility in accommodating high-molecular weight substrates,[27] in the case of *m*-xylene-$^2H_3$ it also exhibits a binding region near the active oxidizing species that limits substrate dynamics of a low-molecular weight substrate. The binding of multiple xylene ligands also contributes to obstructed substrate dynamics; results from the heterotropic experiments indicate that the presence of *p*-xylene modulates the motion of *m*-xylene-$^2H_3$ substrates that have access to the catalytic center. Experiments with labeled and unlabeled *p*-xylene indicate that *p*-xylene and *m*-xylene-$^2H_3$ do not have simultaneous access to the active oxidizing species. The rationale for these conclusions is described subsequently.

Results from the homotropic experiments indicate that the binding region near the active oxidizing species in CYP3A4 is rigid with *m*-xylene-$^2H_3$ as the substrate. Figure 1 shows three of many conceivable orientations of *m*-xylene-$^2H_3$ in the proximity of the active oxidizing species, one that would lead to benzylic hydroxylation at the deuterium-labeled methyl group (i.e., k_{45D}), another that would result in aromatic hydroxylation (k_{46}), and finally an orientation that would result in benzylic hydroxylation at the unlabeled methyl group (k_{45H}). Of the three sites, benzylic hydroxylation at the unlabeled methyl group is favored in the absence of steric factors associated with substrate binding. Compared to aromatic hydroxylation, benzylic positions are generally more reactive and more susceptible to hydroxylation.[45,60,61] Benzylic hydroxylation allows for resonance stabilization of the transition state, while aromatic hydroxylation leads to an intermediate that involves a loss of aromaticity (i.e., arene oxide formation).[62] Thus, when the substrate is reorienting and presenting potential oxidation sites to the active oxidizing species, it is predicted that benzylic hydroxylation at the unlabeled methyl group would be preferred. However, aromatic hydroxylation was preferred in CYP3A4, and the product ratio (2,4-dimethylphenol/*m*-methylbenzyl alcohol) increased with substrate concentration; the $(k_H/k_D)_{obs}$ values increased with product ratio. Aromatic hydroxylation (k_{46}) is a branching route that would lead to $(k_H/k_D)_{obs}$ values that approach the intrinsic isotope effect (Scheme 1 and eq 1), and thus, k_{46} is the major contributor to the increase in $(k_H/k_D)_{obs}$ values. If the reorientation rate, k_{43}, was increasing as a function of substrate concentration, it would be expected that benzylic hydroxylation, rather than aromatic hydroxylation, would become more favored with an increasing substrate concentration.

To the best of our knowledge, CYP3A4's preference for aromatic hydroxylation of *m*-xylene-$^2H_3$ and, albeit to a lower but still notable degree with *p*-xylene, is unprecedented in regard to xylene metabolism.[37,38,44,45,47] Xylene isomers are metabolized predominantly through benzylic hydroxylation, with 95% eliminated as the conjugate of the downstream carboxylic acid,[63] and overall, benzylic hydroxylation has been overwhelmingly preferred over aromatic hydroxylation in studies that have utilized the intramolecular isotope effect design. Selectivity for aromatic hydroxylation is particularly interesting when it is compared to the results of previous studies with *m*-xylene-$^2H_3$ involving CYP2E1 and CYP2A6. In those studies, *m*-methylbenzyl alcohol was indisputably the favored product; *m*-methylbenzyl alcohol was preferred over 2,4-dimethylphenol 19.3 to 1 for CYP2E1 and 4.8 to 1 for CYP2A6.[44] Moreover, the metabolism of *p*-xylene-$^2H_3$ by CYP2E1, CYP2A6, and phenobarbital-induced microsomes was overwhelmingly selective for benzylic hydroxylation over aromatic hydroxylation: *p*-methylbenzyl alcohol represented 95% of the product formed from phenobarbital-induced microsomes and was the only product detected from CYP2E1- and CYP2A6-mediated metabolism.[37,44] In this study, aromatic hydroxylation represented 26% of the product formed from CYP3A4-mediated oxidation of *p*-xylene. CYP2E1 and CYP2A6 isoforms exhibit profoundly smaller active site volumes in comparison to that of CYP3A4.[27,64,65] The voluminous and flexible CYP3A4 active site would be expected to easily accommodate *m*-xylene-$^2H_3$ and permit sufficient substrate motion, so that the most favorable site of metabolism is positioned near the active oxidizing species and therefore would display product selectivity for *m*-methylbenzyl alcohol. The selectivity for aromatic hydroxylation by CYP3A4 indicates that substrate motion is hindered to the point that the rate of reorientation is, on average, slower than the rate of oxidation.

The heterotropic studies presented here indicate that *p*-xylene is an allosteric effector of interactions between CYP3A4 and *m*-xylene-$^2H_3$ substrates and suggest that *p*-xylene, as the effector molecule, influences product selectivity by modulating substrate motion. It has been shown that steric constraints modulate the rate of reorientation between labeled and unlabeled groups and, therefore, the value of $(k_H/k_D)_{obs}$ in intramolecular isotope effect experiments.[37,38,46] Moreover, site-directed mutagenesis to generate a more spacious active site led to increased $(k_H/k_D)_{obs}$ values compared to that of the wild-type enzyme.[47] In the study presented here, the $(k_H/k_D)_{obs}$ values for *m*-xylene-$^2H_3$ hydroxylation decreased as a function of *p*-xylene concentration, indicating that the rate of reorientation of *m*-xylene-$^2H_3$ was slowed by the presence of *p*-xylene.

Uncoupling is a form of branching and will lead to increased $(k_H/k_D)_{obs}$ values similar to production of $P2_H$.[57,66] Therefore,

it is reasonable to consider that improved coupling efficiency contributes to the *p*-xylene-dependent decrease in $(k_H/k_D)_{obs}$ for *m*-xylene-$^2H_3$ oxidation. If this was the case, improved coupling would be reflected in increased rates of product formation from *m*-xylene-$^2H_3$ hydroxylation, which were not observed (Figure 9 and Table 1). Improved coupling could potentially lead to enhanced *p*-xylene oxidation rather than *m*-xylene-$^2H_3$ oxidation. If both molecules have simultaneous access to the active oxidizing species, this would represent another form of branching from benzylic hydroxylation of *m*-xylene-$^2H_3$, in which the active oxidizing species may partake. However, this scenario would generate higher $(k_H/k_D)_{obs}$ values for *m*-xylene-$^2H_3$ oxidation rather than the decreasing trend observed here. Moreover, the heterotropic experiments indicate that *p*-xylene and *m*-xylene-$^2H_3$ do not have simultaneous access to the active oxidizing species (see below). Overall, the results and existing models that describe how $(k_H/k_D)_{obs}$ is modulated by branching routes do not support a significant role for the *p*-xylene-induced improvement in coupling efficiency as a source for the decrease in $(k_H/k_D)_{obs}$ for *m*-xylene-$^2H_3$ oxidation. Interestingly, other studies of CYP3A4 have shown that oxidase activity increased with substrate/effector concentration.[67]

The biphasic kinetic curves (Figures 3 and 8) in homotropic experiments, the increase in the product ratio as a function of *m*-xylene-$^2H_3$ concentration (Figure 5), and the observation that *p*-xylene acts as a modulator of *m*-xylene-$^2H_3$ motion (Figure 9 and Table 1) are all examples of allosteric behavior. The mechanistic basis for CYP allosteric behavior has been reviewed,[5,9,20] and the current models include multiple-ligand binding,[27] conformational selection,[68] and protein−protein interactions.[19,22,69] An amalgamation of mechanisms has also been proposed.[19,20]

Interpretation of the results using the multiple-ligand binding model of allosteric behavior would involve multiple xylene ligands binding simultaneously within the active site or at least one substrate in the active site and another ligand at a peripheral binding site that modulates the active site space by prompting conformational changes. Crystal structures show that the CYP3A4 active site accommodates substrates as large as erythromycin (734 Da) or, in another instance, two ketoconazole molecules (531 Da) simultaneously,[27] so it is reasonable that the active site could accommodate at least two xylene molecules (106 Da).

Figure 10 shows two examples of how multiple xylene molecules could bind simultaneously within the active site. In one scenario, *m*-xylene-$^2H_3$ and *p*-xylene both have access to the active oxidizing species simultaneously and are, in essence, "competing" for oxidation. In this "shared-access" model, several potential oxidation sites on both ligands could be presented to the active oxidizing species on a time scale that is faster than the oxidative step. In this scenario, it is expected that products generated from oxidation at more reactive sites (e.g., benzylic carbons) would be preferred.[45,61] Alternatively, the molecules may bind such that only one molecule has access to the active oxidizing species, for example, in a stacked fashion. In this scenario, only the molecule closest to the heme (i.e., *m*-xylene-$^2H_3$) could act as the substrate while the molecule farthest from the heme (i.e., *p*-xylene) could still modulate the rate of reorientation of the substrate molecule. Stacked binding has been observed in crystal structures of CYP3A4[27] and P450eryF.[23] There are also examples of small molecules

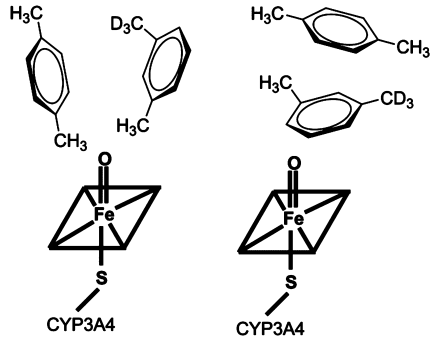

Figure 10. Two hypothetical scenarios of how two xylene molecules may bind near catalytic species in CYP3A4. On the left, *p*-xylene and *m*-xylene-$^2H_3$ have simultaneous access to the active oxidizing species. On the right, only *m*-xylene-$^2H_3$ has access as the substrate and effector bind in a stacked fashion.

interacting with CYP enzymes in regions other than the substrate binding site.[9,20,24]

Within the framework of the multiple-ligand model, the results support a scenario in which a single molecule has access to the active oxidizing species rather than the shared-access scenario. In the heterotropic experiments, *p*-xylene-$^2H_6$ and unlabeled *p*-xylene had similar effects on *m*-xylene-$^2H_3$ motion. Both effector molecules modulated a decrease in the extent of *m*-xylene-$^2H_3$ motion as evidenced by a concentration-dependent decrease in $(k_H/k_D)_{obs}$ for *m*-xylene-$^2H_3$ oxidation and exhibited similar product ratios. If *m*-xylene-$^2H_3$ and *p*-xylene have simultaneous access to the active oxidizing species (Figure 11), labeled and unlabeled *p*-xylene would exhibit dissimilar effects on the $(k_H/k_D)_{obs}$ values and/or the product ratio for *m*-xylene-$^2H_3$ oxidation. The methyl groups in unlabeled *p*-xylene are favorable sites for oxidation. In a situation in which *m*-xylene-$^2H_3$ is oriented so that less favorable sites for oxidation

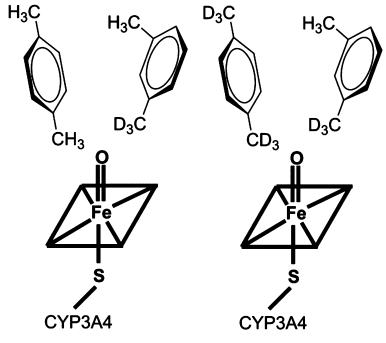

Figure 11. Scenarios displaying how unlabeled and deuterium-labeled *p*-xylene exhibit dissimilar effects on *m*-xylene-$^2H_3$ oxidation when *para* and *meta* isomers have simultaneous access to the active oxidizing species. In the image on the left, when *m*-xylene-$^2H_3$ is oriented with the deuterium-labeled methyl group toward the active oxidizing species, an unlabeled methyl group on *p*-xylene is available for oxidation. When deuterium-labeled *p*-xylene replaces unlabeled *p*-xylene, there are no longer favorable sites for oxidation readily available. Thus, oxidation at the deuterium-labeled methyl group of *m*-xylene-$^2H_3$ would generate lower $(k_H/k_D)_{obs}$ values. Alternatively, the active oxidizing species could hydroxylate the aromatic ring of *m*-xylene-$^2H_3$ or the aromatic ring of *p*-xylene-$^2H_6$ or uncouple to generate H_2O. Any of these would increase $(k_H/k_D)_{obs}$ values (Scheme 1 and eq 1). An increased level of hydroxylation of the *m*-xylene-$^2H_3$ aromatic ring would be detected as an increase in the 2,4-dimethylphenol/*m*-methylbenzyl alcohol product ratio.

dx.doi.org/10.1021/bi401472p | *Biochemistry* 2014, 53, 1018−1028

are presented to the active oxidizing species (i.e., the deuterium-labeled methyl group or the aromatic ring), oxidation at the benzylic carbons in unlabeled *p*-xylene should be favored. When deuterium-labeled *p*-xylene is the effector molecule, the benzylic carbons of *p*-xylene are not more favorable than the deuterium-labeled carbon of *m*-xylene-$^2H_3$ or a carbon that is part of the aromatic ring. Thus, if *p*-xylene and *m*-xylene-$^2H_3$ have simultaneous access to the active oxidizing species, then, in comparison to that of unlabeled *p*-xylene, deuterium-labeled *p*-xylene would generate a more profound decrease in $(k_H/k_D)_{obs}$ for *m*-xylene-$^2H_3$ oxidation or an increased level of formation of 2,4-dimethylphenol, that is, an increase in the product ratio. Consistent with this, previous studies showed that deuterium-labeled effector molecules displayed dramatic differences in the product ratio in comparison to unlabeled effector molecules, and it was concluded that the effector and substrate occupy the active site simultaneously.[43,44] In contrast, our results show similar product ratios with labeled and unlabeled effector molecules.

The results from the homotropic experiments, when *m*-xylene-$^2H_3$ acts as both the effector and the substrate, are also more consistent with a scenario in which only a single molecule has access to the active oxidizing species. In the shared-access model, two *m*-xylene-$^2H_3$ molecules would have simultaneous access to the active oxidizing species, increasing the likelihood of oxidation of one of the unlabeled benzylic carbons; *m*-methylbenzyl alcohol would be the more preferred product rather than 2,4-dimethylphenol. However, in the homotropic experiments, the preferred product was 2,4-dimethylphenol. Another reasonable explanation for hindered substrate motion is that there are more than two xylene molecules bound simultaneously to the CYP3A4 active site. In this scenario, the obstruction of *m*-xylene-$^2H_3$ motion near the catalytic center would be due to several xylene ligands binding in the active site, and the packing of molecules generates a substrate binding orientation that on average favors aromatic hydroxylation. While it would be expected that CYP3A4's voluminous active site could readily accommodate more than two xylene ligands,[27] the preference for aromatic hydroxylation is observed even at *m*-xylene-$^2H_3$ concentrations below the K_{m1}. This evidence is more supportive of protein motion restricting substrate motion above the active oxidizing species rather than the packing of xylene molecules.

In the context of the conformational selectivity model, the preference for aromatic hydroxylation would indicate that multiple CYP3A4 conformers exist, one that is selective for aromatic hydroxylation and the other that is selective for benzylic hydroxylation. In this model, the results would indicate that there is a greater population of conformers selective for aromatic hydroxylation of *m*-xylene-$^2H_3$ compared to the population of conformers selective for benzylic hydroxylation. With this model, the results suggest that it is the conformer that is selective for aromatic hydroxylation that restricts substrate motion in the region above the catalytic center. Active site waters may also contribute to the product selectivity[26,48] but were not a focus of this study.

While both the heterotropic and homotropic experiments support a binding scenario in which the substrate and effector do not have simultaneous access to the oxidizing species, the binding location(s) of the effector and mechanisms by which the effector modulates substrate dyanmics are less clear and cannot distinguish whether, for instance, the effector molecules bind in a stacked fashion as shown in Figure 10 or at a more distant or peripheral site. Binding to this more distant site could reduce the available active site volume either by generating a structural change in the enzyme or more simply by occupying the space so that less volume is available for the substrate. The heterotropic experiments with unlabeled and labeled *p*-xylene show that the turnover of *m*-xylene-$^2H_3$ is not inhibited by the presence of the effector molecules. Moreover, the 2,4-dimethylphenol/*m*-methylbenzyl alcohol product ratio was stable across the effector concentration range (Figure 9). Therefore, overall, the presence of *p*-xylene effector molecules generated a decrease in the level of *m*-xylene-$^2H_3$ substrate motion without profoundly impacting the rate of turnover or reaction selectivity (i.e., aromatic vs benzylic hydroxylation). These data support a model in which *p*-xylene binds at a site that is unique from the site where *m*-xylene-$^2H_3$ binds when it is a substrate. On the basis of the respective K_{m1} values for *p*-xylene and *m*-xylene-$^2H_3$, it would be expected that inhibition of *m*-xylene-$^2H_3$ oxidation would occur at *p*-xylene concentrations of >60 μM if both molecules competed for the same binding site.

On the basis of the evidence currently available, a reasonable "effector" binding site for *p*-xylene is the "phenylalanine cluster" observed in the crystal structure of CYP3A4.[24] The surprisingly small active site volume of CYP3A4 in this crystal structure was attributed to this group of phenylalanine residues. Further evidence of the region's flexibility was reported in the CYP3A4 crystal structure with two ketoconazoles bound to the active site,[27] and prior to the publication of these crystal structures, mutagenesis pointed to their role in CYP3A4 cooperative behavior.[70−72] More recently, a study involving fluorescence resonance energy transfer, mutagenesis, and molecular modeling further implicated this region as a peripheral binding site.[25] As an aromatic molecule capable of π-stacking interactions, it follows chemical logic that a phenylalanine cluster is a favorable potential site for *p*-xylene binding. However, if this is the case, the results from this study indicate that the flexibility of this region in forming a "closed" conformation is much greater than observed previously with metyrapone.[24]

In conclusion, this study has provided evidence of allosteric behavior in CYP3A4-mediated *p*-xylene and *m*-xylene-$^2H_3$ hydroxylation and new mechanistic details of CYP3A4 allosteric behavior by showing that a heterotropic effector, *p*-xylene, modulates substrate motion, that is, *m*-xylene-$^2H_3$ dynamics. While this method has been utilized to study the allosteric behavior of other CYP isoforms,[44] we believe this is the first time it has been used to study an isoform with evidence of allosteric phenomena as extensive as that for CYP3A4. The evidence supports a model in which the CYP3A4 active site exhibits sufficient conformational diversity not only to accommodate high-molecular weight substrates but also to generate a substrate binding site that hinders substrate motion for substrates even as small as *m*-xylene-$^2H_3$, as shown by selectivity for aromatic hydroxylation over benzylic hydroxylation. The techniques available for studying substrate motion when the enzyme is in an activated state are limited. The mounting evidence indicates that ligand binding and allosteric mechanisms can be profoundly complex and involve multiple factors.[19,20,22,48−51,67] This work indicates that the intramolecular isotope effect experimental design offers the opportunity to discern whether an allosteric mechanism involves ligand-induced modulation of substrate motion and, thus, could be paired with other biophysical techniques and *in*

vitro systems to generate a more complete picture of CYP allosterism.

■ ASSOCIATED CONTENT

Supporting Information

Representative standard curves used for quantification of *m*-methylbenzyl alcohol, *p*-methylbenzyl alcohol, 2,4-dimethylphenol, and 2,5-dimethylphenol; product formation rates of CYP3A4-mediated *p*-xylene oxidation fit to a biphasic kinetic model; and representative GC−MS traces from homotropic and heterotropic experiments with *m*-xylene-$^2H_3$ and *p*-xylene. This material is available free of charge via the Internet at http://pubs.acs.org.

■ AUTHOR INFORMATION

Corresponding Author

*School of Pharmacy, Pacific University Oregon, Hillsboro, OR 97123. E-mail: harrelsonj@pacificu.edu. Telephone: (503) 352-7292. Fax: (503) 352-7270.

Present Address

§W.K.C.: Department of Surgery, Pinnacle Health System, Harrisburg, PA 17104.

Funding

This research was supported by funds provided by Pacific University Oregon.

Notes

The authors declare no competing financial interest.

■ ACKNOWLEDGMENTS

We thank James Currie for his assistance with the GC−MS experiments and Ryan Seguin for providing recommendations during a review of the manuscript.

■ ABBREVIATIONS

CYP or P450, cytochrome P450; k_H/k_D, intrinsic isotope effect; $(k_H/k_D)_{obs}$, measured isotope effect; MBA, methylbenzyl alcohol; 2,4-DMP, 2,4-dimethylphenol; 2,5-DMP, 2,5-dimethylphenol.

■ REFERENCES

(1) Guengerich, F. P. (2001) Common and uncommon cytochrome P450 reactions related to metabolism and chemical toxicity. *Chem. Res. Toxicol. 14*, 611−650.

(2) Isin, E. M., and Guengerich, F. P. (2007) Complex reactions catalyzed by cytochrome P450 enzymes. *Biochim. Biophys. Acta 1770*, 314−329.

(3) Yang, J., Atkins, W. M., Isoherranen, N., Paine, M. F., and Thummel, K. E. (2012) Evidence of CYP3A allosterism in vivo: Analysis of interaction between fluconazole and midazolam. *Clin. Pharmacol. Ther. 91*, 442−449.

(4) Chen, W., Koenigs, L. L., Thompson, S. J., Peter, R. M., Rettie, A. E., Trager, W. F., and Nelson, S. D. (1998) Oxidation of acetaminophen to its toxic quinone imine and nontoxic catechol metabolites by baculovirus-expressed and purified human cytochromes P450 2E1 and 2A6. *Chem. Res. Toxicol. 11*, 295−301.

(5) Atkins, W. M. (2005) Non-Michaelis-Menten kinetics in cytochrome P450-catalyzed reactions. *Annu. Rev. Pharmacol. Toxicol. 45*, 291−310.

(6) Huang, M. T., Chang, R. L., Fortner, J. G., and Conney, A. H. (1981) Studies on the mechanism of activation of microsomal benzo[a]pyrene hydroxylation by flavonoids. *J. Biol. Chem. 256*, 6829−6836.

(7) Lasker, J. M., Huang, M. T., and Conney, A. H. (1982) In vivo activation of zoxazolamine metabolism by flavone. *Science 216*, 1419−1421.

(8) Schwab, G. E., Raucy, J. L., and Johnson, E. F. (1988) Modulation of rabbit and human hepatic cytochrome P-450-catalyzed steroid hydroxylations by α-naphthoflavone. *Mol. Pharmacol. 33*, 493−499.

(9) Denisov, I. G., and Sligar, S. G. (2012) A novel type of allosteric regulation: Functional cooperativity in monomeric proteins. *Arch. Biochem. Biophys. 519*, 91−102.

(10) Stresser, D. M., Blanchard, A. P., Turner, S. D., Erve, J. C., Dandeneau, A. A., Miller, V. P., and Crespi, C. L. (2000) Substrate-dependent modulation of CYP3A4 catalytic activity: Analysis of 27 test compounds with four fluorometric substrates. *Drug Metab. Dispos. 28*, 1440−1448.

(11) Jones, J. P. (2004) Metabolic menages a trois: What does it mean for drug design? *Drug Discovery Today 9*, 592.

(12) Tang, W., Stearns, R. A., Kwei, G. Y., Iliff, S. A., Miller, R. R., Egan, M. A., Yu, N. X., Dean, D. C., Kumar, S., Shou, M., Lin, J. H., and Baillie, T. A. (1999) Interaction of diclofenac and quinidine in monkeys: Stimulation of diclofenac metabolism. *J. Pharmacol. Exp. Ther. 291*, 1068−1074.

(13) Blobaum, A. L., Bridges, T. M., Byers, F. W., Turlington, M., Mattmann, M., Morrison, R. D., Mackie, C., Lavreysen, H., Bartolome, J. M., Macdonald, G. J., Steckler, T., Jones, C. K., Niswender, C. M., Conn, P. J., Lindsley, C. W., Stauffer, S. R., and Daniels, J. S. (2013) Heterotropic Activation of the Midazolam Hydroxylase Activity of CYP3A by a Positive Allosteric Modulator of mGlu5: In Vitro to In Vivo Translation and Potential Impact on Clinically Relevant Drug-Drug Interactions. *Drug Metab. Dispos. 41*, 2066−2075.

(14) Hutzler, J. M., Frye, R. F., Korzekwa, K. R., Branch, R. A., Huang, S. M., and Tracy, T. S. (2001) Minimal in vivo activation of CYP2C9-mediated flurbiprofen metabolism by dapsone. *Eur. J. Pharm. Sci. 14*, 47−52.

(15) Egnell, A. C., Houston, B., and Boyer, S. (2003) In vivo CYP3A4 heteroactivation is a possible mechanism for the drug interaction between felbamate and carbamazepine. *J. Pharmacol. Exp. Ther. 305*, 1251−1262.

(16) Wienkers, L. C., and Heath, T. G. (2005) Predicting in vivo drug interactions from in vitro drug discovery data. *Nat. Rev. Drug Discovery 4*, 825−833.

(17) Houston, J. B., and Kenworthy, K. E. (2000) In vitro-in vivo scaling of CYP kinetic data not consistent with the classical Michaelis-Menten model. *Drug Metab. Dispos. 28*, 246−254.

(18) Obach, R. S. (2012) Heterotropic effects on drug-metabolizing enzyme activities: In vitro curiosity emerges as a clinically meaningful phenomenon (perhaps?). *Clin. Pharmacol. Ther. 91*, 385−387.

(19) Davydov, D. R. (2011) Microsomal monooxygenase as a multienzyme system: The role of P450-P450 interactions. *Expert Opin. Drug Metab. Toxicol. 7*, 543−558.

(20) Davydov, D. R., and Halpert, J. R. (2008) Allosteric P450 mechanisms: Multiple binding sites, multiple conformers or both? *Expert Opin. Drug Metab. Toxicol. 4*, 1523−1535.

(21) Schrag, M. L., and Wienkers, L. C. (2000) Topological alteration of the CYP3A4 active site by the divalent cation Mg^{2+}. *Drug Metab. Dispos. 28*, 1198−1201.

(22) Reed, J. R., Cawley, G. F., and Backes, W. L. (2013) Interactions between cytochromes P450 2B4 (CYP2B4) and 1A2 (CYP1A2) lead to alterations in toluene disposition and P450 uncoupling. *Biochemistry 52*, 4003−4013.

(23) Cupp-Vickery, J., Anderson, R., and Hatziris, Z. (2000) Crystal structures of ligand complexes of P450eryF exhibiting homotropic cooperativity. *Proc. Natl. Acad. Sci. U.S.A. 97*, 3050−3055.

(24) Williams, P. A., Cosme, J., Vinkovic, D. M., Ward, A., Angove, H. C., Day, P. J., Vonrhein, C., Tickle, I. J., and Jhoti, H. (2004) Crystal structures of human cytochrome P450 3A4 bound to metyrapone and progesterone. *Science 305*, 683−686.

(25) Davydov, D. R., Rumfeldt, J. A., Sineva, E. V., Fernando, H., Davydova, N. Y., and Halpert, J. R. (2012) Peripheral ligand-binding

site in cytochrome P450 3A4 located with fluorescence resonance energy transfer (FRET). *J. Biol. Chem. 287*, 6797−6809.
(26) Skopalik, J., Anzenbacher, P., and Otyepka, M. (2008) Flexibility of human cytochromes P450: Molecular dynamics reveals differences between CYPs 3A4, 2C9, and 2A6, which correlate with their substrate preferences. *J. Phys. Chem. B 112*, 8165−8173.
(27) Ekroos, M., and Sjogren, T. (2006) Structural basis for ligand promiscuity in cytochrome P450 3A4. *Proc. Natl. Acad. Sci. U.S.A. 103*, 13682−13687.
(28) Williams, P. A., Cosme, J., Ward, A., Angove, H. C., Matak Vinkovic, D., and Jhoti, H. (2003) Crystal structure of human cytochrome P450 2C9 with bound warfarin. *Nature 424*, 464−468.
(29) Wilderman, P. R., Shah, M. B., Jang, H. H., Stout, C. D., and Halpert, J. R. (2013) Structural and thermodynamic basis of (+)-α-pinene binding to human cytochrome P450 2B6. *J. Am. Chem. Soc. 135*, 10433−10440.
(30) Brandman, R., Lampe, J. N., Brandman, Y., and de Montellano, P. R. (2011) Active-site residues move independently from the rest of the protein in a 200 ns molecular dynamics simulation of cytochrome P450 CYP119. *Arch. Biochem. Biophys. 509*, 127−132.
(31) Scott, E. E., He, Y. A., Wester, M. R., White, M. A., Chin, C. C., Halpert, J. R., Johnson, E. F., and Stout, C. D. (2003) An open conformation of mammalian cytochrome P450 2B4 at 1.6-Å resolution. *Proc. Natl. Acad. Sci. U.S.A. 100*, 13196−13201.
(32) Scott, E. E., White, M. A., He, Y. A., Johnson, E. F., Stout, C. D., and Halpert, J. R. (2004) Structure of mammalian cytochrome P450 2B4 complexed with 4-(4-chlorophenyl)imidazole at 1.9-Å resolution: Insight into the range of P450 conformations and the coordination of redox partner binding. *J. Biol. Chem. 279*, 27294−27301.
(33) Wilderman, P. R., Shah, M. B., Liu, T., Li, S., Hsu, S., Roberts, A. G., Goodlett, D. R., Zhang, Q., Woods, V. L., Jr., Stout, C. D., and Halpert, J. R. (2010) Plasticity of cytochrome P450 2B4 as investigated by hydrogen-deuterium exchange mass spectrometry and X-ray crystallography. *J. Biol. Chem. 285*, 38602−38611.
(34) Lee, H., Ortiz de Montellano, P. R., and McDermott, A. E. (1999) Deuterium magic angle spinning studies of substrates bound to cytochrome P450. *Biochemistry 38*, 10808−10813.
(35) Isin, E. M., and Guengerich, F. P. (2006) Kinetics and thermodynamics of ligand binding by cytochrome P450 3A4. *J. Biol. Chem. 281*, 9127−9136.
(36) Isin, E. M., and Guengerich, F. P. (2007) Multiple sequential steps involved in the binding of inhibitors to cytochrome P450 3A4. *J. Biol. Chem. 282*, 6863−6874.
(37) Iyer, K. R., Jones, J. P., Darbyshire, J. F., and Trager, W. F. (1997) Intramolecular isotope effects for benzylic hydroxylation of isomeric xylenes and 4,4′-dimethylbiphenyl by cytochrome P450: Relationship between distance of methyl groups and masking of the intrinsic isotope effect. *Biochemistry 36*, 7136−7143.
(38) Henne, K. R., Fisher, M. B., Iyer, K. R., Lang, D. H., Trager, W. F., and Rettie, A. E. (2001) Active site characteristics of CYP4B1 probed with aromatic ligands. *Biochemistry 40*, 8597−8605.
(39) Nelson, S. D., and Trager, W. F. (2003) The use of deuterium isotope effects to probe the active site properties, mechanism of cytochrome P450-catalyzed reactions, and mechanisms of metabolically dependent toxicity. *Drug Metab. Dispos. 31*, 1481−1498.
(40) Hjelmeland, L. M., Aronow, L., and Trudell, J. R. (1977) Intramolecular determination of substituent effects in hydroxylations catalyzed by cytochrome P-450. *Mol. Pharmacol. 13*, 634−639.
(41) Miwa, G. T., Garland, W. A., Hodshon, B. J., Lu, A. Y., and Northrop, D. B. (1980) Kinetic isotope effects in cytochrome P-450-catalyzed oxidation reactions. Intermolecular and intramolecular deuterium isotope effects during the N-demethylation of N,N-dimethylphentermine. *J. Biol. Chem. 255*, 6049−6054.
(42) Gelb, M. H., Heimbrook, D. C., Malkonen, P., and Sligar, S. G. (1982) Stereochemistry and deuterium isotope effects in camphor hydroxylation by the cytochrome P450cam monoxygenase system. *Biochemistry 21*, 370−377.
(43) Rock, D. A., Perkins, B. N., Wahlstrom, J., and Jones, J. P. (2003) A method for determining two substrates binding in the same active site of cytochrome P450BM3: An explanation of high energy omega product formation. *Arch. Biochem. Biophys. 416*, 9−16.
(44) Harrelson, J. P., Atkins, W. M., and Nelson, S. D. (2008) Multiple-ligand binding in CYP2A6: Probing mechanisms of cytochrome P450 cooperativity by assessing substrate dynamics. *Biochemistry 47*, 2978−2988.
(45) Hanzlik, R. P., and Ling, K. H. J. (1993) Active-site dynamics of xylene hydroxylation by cytochrome-P-450 as revealed by kinetic deuterium-isotope effects. *J. Am. Chem. Soc. 115*, 9363−9370.
(46) Harrelson, J. P., Henne, K. R., Alonso, D. O., and Nelson, S. D. (2007) A comparison of substrate dynamics in human CYP2E1 and CYP2A6. *Biochem. Biophys. Res. Commun. 352*, 843−849.
(47) Rock, D. A., Boitano, A. E., Wahlstrom, J. L., and Jones, J. P. (2002) Use of kinetic isotope effects to delineate the role of phenylalanine 87 in P450(BM-3). *Bioorg. Chem. 30*, 107−118.
(48) Conner, K. P., Vennam, P., Woods, C. M., Krzyaniak, M. D., Bowman, M. K., and Atkins, W. M. (2012) 1,2,3-Triazole-heme interactions in cytochrome P450: Functionally competent triazole-water-heme complexes. *Biochemistry 51*, 6441−6457.
(49) Woods, C. M., Fernandez, C., Kunze, K. L., and Atkins, W. M. (2011) Allosteric activation of cytochrome P450 3A4 by α-naphthoflavone: Branch point regulation revealed by isotope dilution analysis. *Biochemistry 50*, 10041−10051.
(50) Guengerich, F. P., Sohl, C. D., and Chowdhury, G. (2011) Multi-step oxidations catalyzed by cytochrome P450 enzymes: Processive vs. distributive kinetics and the issue of carbonyl oxidation in chemical mechanisms. *Arch. Biochem. Biophys. 507*, 126−134.
(51) Roberts, A. G., Campbell, A. P., and Atkins, W. M. (2005) The thermodynamic landscape of testosterone binding to cytochrome P450 3A4: Ligand binding and spin state. *Biochemistry 44*, 1353−1366.
(52) Cameron, M. D., Wen, B., Roberts, A. G., Atkins, W. M., Campbell, A. P., and Nelson, S. D. (2007) Cooperative binding of acetaminophen and caffeine within the P450 3A4 active site. *Chem. Res. Toxicol. 20*, 1434−1441.
(53) Ghose, A. K., Viswanadhan, V. N., and Wendoloski, J. J. (1999) A knowledge-based approach in designing combinatorial or medicinal chemistry libraries for drug discovery. 1. A qualitative and quantitative characterization of known drug databases. *ACS Comb. Sci. 1*, 55−68.
(54) Ueng, Y. F., Kuwabara, T., Chun, Y. J., and Guengerich, F. P. (1997) Cooperativity in oxidations catalyzed by cytochrome P450 3A4. *Biochemistry 36*, 370−381.
(55) Khan, K. K., He, Y. Q., Domanski, T. L., and Halpert, J. R. (2002) Midazolam oxidation by cytochrome P450 3A4 and active-site mutants: An evaluation of multiple binding sites and of the metabolic pathway that leads to enzyme inactivation. *Mol. Pharmacol. 61*, 495−506.
(56) Korzekwa, K. R., Krishnamachary, N., Shou, M., Ogai, A., Parise, R. A., Rettie, A. E., Gonzalez, F. J., and Tracy, T. S. (1998) Evaluation of atypical cytochrome P450 kinetics with two-substrate models: Evidence that multiple substrates can simultaneously bind to cytochrome P450 active sites. *Biochemistry 37*, 4137−4147.
(57) Korzekwa, K. R., Trager, W. F., and Gillette, J. R. (1989) Theory for the observed isotope effects from enzymatic systems that form multiple products via branched reaction pathways: Cytochrome P-450. *Biochemistry 28*, 9012−9018.
(58) Harada, N., Miwa, G. T., Walsh, J. S., and Lu, A. Y. (1984) Kinetic isotope effects on cytochrome P-450-catalyzed oxidation reactions. Evidence for the irreversible formation of an activated oxygen intermediate of cytochrome P-448. *J. Biol. Chem. 259*, 3005−3010.
(59) Jones, J. P., Korzekwa, K. R., Rettie, A. E., and Trager, W. F. (1986) Isotopically Sensitive Branching and Its Effect on the Observed Intramolecular Isotope Effects in Cytochrome-P-450 Catalyzed-Reactions: A New Method for the Estimation of Intrinsic Isotope Effects. *J. Am. Chem. Soc. 108*, 7074−7078.
(60) Ling, K. H., and Hanzlik, R. P. (1989) Deuterium isotope effects on toluene metabolism. Product release as a rate-limiting step in cytochrome P-450 catalysis. *Biochem. Biophys. Res. Commun. 160*, 844−849.

(61) Hanzlik, R. P., and Ling, K. H. J. (1990) Active-site dynamics of toluene hydroxylation by cytochrome-P-450. *J. Org. Chem. 55*, 3992−3997.
(62) Jerina, D. M., and Daly, J. W. (1974) Arene oxides: A new aspect of drug metabolism. *Science 185*, 573−582.
(63) Langman, J. M. (1994) Xylene: Its toxicity, measurement of exposure levels, absorption, metabolism and clearance. *Pathology 26*, 301−309.
(64) Porubsky, P. R., Meneely, K. M., and Scott, E. E. (2008) Structures of human cytochrome P-450 2E1. Insights into the binding of inhibitors and both small molecular weight and fatty acid substrates. *J. Biol. Chem. 283*, 33698−33707.
(65) Yano, J. K., Hsu, M. H., Griffin, K. J., Stout, C. D., and Johnson, E. F. (2005) Structures of human microsomal cytochrome P450 2A6 complexed with coumarin and methoxsalen. *Nat. Struct. Mol. Biol. 12*, 822−823.
(66) Atkins, W. M., and Sligar, S. G. (1987) Metabolic switching in cytochrome-P-450cam: Deuterium-isotope effects on regiospecificity and the monooxygenase oxidase ratio. *J. Am. Chem. Soc. 109*, 3754−3760.
(67) Grinkova, Y. V., Denisov, I. G., McLean, M. A., and Sligar, S. G. (2013) Oxidase uncoupling in heme monooxygenases: Human cytochrome P450 CYP3A4 in Nanodiscs. *Biochem. Biophys. Res. Commun. 430*, 1223−1227.
(68) Koley, A. P., Buters, J. T., Robinson, R. C., Markowitz, A., and Friedman, F. K. (1997) Differential mechanisms of cytochrome P450 inhibition and activation by α-naphthoflavone. *J. Biol. Chem. 272*, 3149−3152.
(69) Reed, J. R., Connick, J. P., Cheng, D., Cawley, G. F., and Backes, W. L. (2012) Effect of homomeric P450-P450 complexes on P450 function. *Biochem. J. 446*, 489−497.
(70) Harlow, G. R., and Halpert, J. R. (1998) Analysis of human cytochrome P450 3A4 cooperativity: Construction and characterization of a site-directed mutant that displays hyperbolic steroid hydroxylation kinetics. *Proc. Natl. Acad. Sci. U.S.A. 95*, 6636−6641.
(71) Domanski, T. L., He, Y. A., Harlow, G. R., and Halpert, J. R. (2000) Dual role of human cytochrome P450 3A4 residue Phe-304 in substrate specificity and cooperativity. *J. Pharmacol. Exp. Ther. 293*, 585−591.
(72) Domanski, T. L., and Halpert, J. R. (2001) Analysis of mammalian cytochrome P450 structure and function by site-directed mutagenesis. *Curr. Drug Metab. 2*, 117−137.